Particulate-Phase and Gaseous Elemental Mercury Emissions During Biomass Combustion: Controlling Factors and Correlation with Particulate Matter Emissions

ARTICLE *in* ENVIRONMENTAL SCIENCE AND TECHNOLOGY · MARCH 2008

Impact Factor: 5.33 · DOI: 10.1021/es071279n · Source: PubMed

Environ. Sci. Technol. **2008,** *42,* 721–727

Particulate-Phase and Gaseous Elemental Mercury Emissions During Biomass Combustion: Controlling Factors and Correlation with Particulate Matter Emissions

DANIEL OBRIST,*,† HANS MOOSMÜLLER,† ROGER SCHÜRMANN,† L.-W. ANTONY CHEN,† AND SONIA M. KREIDENWEIS‡

Division of Atmospheric Sciences, Desert Research Institute, Reno, Nevada, and Department of Atmospheric Science, Colorado State University, Fort Collins, Colorado

Received May 30, 2007. Revised manuscript received September 19, 2007. Accepted October 6, 2007.

Mercury emissions from wildfires are significant natural sources of atmospheric mercury, but little is known about what controls speciation of emissions important to mercury deposition processes. The goal of this study was to quantify gaseous elemental mercury (GEM) and particulate-phase mercury (PHg) emissions from biomass combustion to identify key factors controlling the speciation. Emissions were characterized in an exhaust stack 17 m above fires using a gaseous mercury analyzer and quartz-fiber filters. Fuels included fresh and air-dried leaves, needles, and branches with different fuel moistures (9−95% of dry weight) and combustion properties (e.g., from <10 to 90% of fire durations characterized by flaming phases). Fuel moisture was the overall driving factor defining emissions, with GEM being the dominant fraction (≥95%) in low moisture fuels and substantial PHg contributions—up to 50% of total mercury emissions—in fresh fuels. High PHg emissions were observed during smoldering combustion whereas flaming-dominated fires showed insignificant PHg emissions. PHg mass emissions were correlated with particulate matter (PM; $r^2 = 0.67$), organic carbon (OC; $r^2 = 0.63$) and sulfur (S; $r^2 = 0.46$) mass emissions, but not with elemental carbon (EC) nor with the total mercury emissions. These data suggest that the formation of PHg involves similar processes as the formation of particulate OC, for example condensation of volatile species onto preexisting smoke particles during cooling and dilution. Based on the observed relationship between PM and OC mass concentrations and published emission inventories, we estimate global PHg emissions by wildfires of 4−5 Mg yr^{-1}.

Introduction

Wildfires are important sources of mercury emissions contributing significantly to the atmospheric mercury load (*1–8*). Global estimates of wildfire-related mercury emissions to the atmosphere vary by an order of magnitude, including 104−526 Mg y^{-1} (*3*), 250−430 Mg yr^{-1} (*4*), 800 Mg yr^{-1} (*9*), 104−853 Mg y^{-1} (*10*), and over 1000 Mg yr^{-1} (*2*). Wildfire-related mercury emissions to the atmosphere originate from the considerable amounts of mercury in biomass and organic matter pools (e.g., foliar mercury concentrations of ∼24 μg kg^{-1}) (*11*) that are almost completely emitted into the atmosphere during biomass burning (3, 10). Wildfires therefore accelerate emission and deposition cycles of mercury between terrestrial ecosystems and the atmosphere (e.g., refs *12* and *13*).

The majority of wildfire related mercury emissions is in the form of gaseous elemental mercury (GEM), but a sizeable fraction can be released as particulate-phase mercury as well (PHg; refs (*3*), (*10*), and (*14*); see below). No significant reactive gaseous mercury (RGM) has been detected in biomass smoke (*10*). The speciation of mercury emissions from biomass combustion has important implications for the fate, transport, and deposition of emissions because GEM has lower deposition velocities (estimated at 0.01 cm sec^{-1} over land) as compared to PHg (0.1 cm s^{-1}) or RGM (0.5 cm s^{-1}; refs *15* and *16*), which will allow GEM to undergo long-range transport (*17*). Evidence for this are observed GEM enriched air masses (up to 0.43 ng m^{-3} enrichment) at the West Coast of the U.S. (*18*) and at the Harvard Forest (*4*) which were attributed to biomass burning in Alaska and Canada, respectively. Emissions occurring as PHg or RGM with shorter residence times are likely to lead to increased deposition loads in proximity to emission sources. Examples for this are observed mercury depletion events in polar regions (*19, 20*) and over halogen-enriched water bodies (*21*), where reactive halogen species oxidize GEM to RGM and PHg leading to increased mercury deposition (*22*).

Previous studies have reported PHg contributions in wildfire smoke ranging from minor fractions (≤1%) in dry fuels to higher PHg contributions in green coniferous needles and deciduous vegetation (up to 13% of total mercury; 3, 10). Similar, field measurements yielded variable percentages of PHg from 3 to 5% in a temperate forest fire as compared to 13% contributions in a boreal wildfire (*14*). It is unclear what causes these considerable differences in speciation as very little information is available how fuel types, plant species, fuel conditions, and combustion properties affect speciation. One aspect which has not received any attention in respect to mercury emissions are the inherent differences in combustion properties during wildfires. For example, biomass burning often includes two distinctive combustion phases, i.e., flaming and smoldering combustion. Flaming combustion is a high temperature combustion process often dominant during the initial part of the combustion process when volatiles are released from the fuel and ignite to form a diffusion flame (*9*). Smoldering combustion, on the other hand, is a lower temperature surface process, and fresh fuels with higher moisture contents are more prone to extended smoldering combustion (*23*) since energy consumption for evaporating water prevents the combustion temperature from reaching the flaming threshold. Smoldering combustion generally leads to increased volatile organic compounds (VOCs) and particulate organic matter (OM) emissions (*23, 24*), but mercury contents of these emissions are lacking.

The goal of this study is to quantify mercury emissions from laboratory combustion of different wildland fuels. We specifically address influences of plant species, fuel types (leaves, needles, branches), fuel moisture levels, combustion properties, and total fuel mercury level on speciation between GEM and PHg emissions. We also evaluate the dependence of PHg emissions on PM mass and composition to infer about

* Corresponding author phone: (775) 674-7008; e-mail: daniel.obrist@dri.edu.
† Desert Research Institute.
‡ Colorado State University.

10.1021/es071279n CCC: $40.75
Published on Web 12/21/2007

TABLE 1. Fuel List of Combustion Experiments. Fuel Moistures Are Expressed in Percent of Dry Mass. Mean Values of Three Burns ± Standard Deviations

burn	species	fuel type	dried/fresh	fuel moisture (%)	mercury conc. (μg/kg)
3	ponderosa pine	needles	air dried	9.8 ± 0.5	24.2 ± 6.6
3	ponderosa pine	needles	air dried	10.3 ± 0.5	28.6 ± 4.3
3	ponderosa pine	needles	fresh	58.7 ± 1.7	12.4 ± 1.5
3	ponderosa pine	small branches	air dried	9.3 ± 0.3	39.2 ± 19.4
3	ponderosa pine	small branches	fresh	46.5 ± 3.6	7.3 ± 1.7
3	ponderosa pine	large branches	air dried	9.3 ± 0.1	26.7 ± 18.5
3	ponderosa pine	large branches	fresh	67.2 ± 4.5	6.0 ± 3.6
3	lodgepole pine	needles	air dried	14.8 ± 1.0	102 ± 16.3
3	lodgepole pine	needles	air dried	22.4 ± 2.0	133.3 ± 17.5
3	lodgepole pine	needles	fresh	83.6 ± 7.1	10.8 ± 1.9
3	lodgepole pine	small branches	air dried	9.1 ± 0.2	38.9 ± 22.6
2	rice	straw	air dried	9.6 ± 0.8	8.8 ± 1.0
3	palmetto	leaves	air dried	10.9 ± 0.9	20.9 ± 9.4
3	chamise	leaves	air dried	15.4 ± 5.8	23.4 ± 2.9
3	chamise	leaves	fresh	56.2 ± 4.0	20.8 ± 7.8
3	chamise	branches	air dried	18.4 ± 1.6	26.2 ±
3	chamise	branches	air dried	33.3 ± 2.2	23.7 ± 14.2
3	chamise	branches	fresh	41.2 ± 15.0	26.8 ± 23.4
3	manzanita	branches	fresh	67.1 ± 3.8	7.8 ± 0.4
3	manzanita	leaves	air dried	55.8 ± 3.7	19.1 ± 1.9
1	manzanita	leaves	fresh	94.5	16.1

mechanisms of PHg formation. This study was conducted at the U.S. Forest Service (USFS) Fire Science Laboratory (FSL) in Missoula, Montana, which allowed for relatively controlled combustion of fuels and detailed characterization of emissions in an exhaust stack 17 m above the fuel bed. Further description of mercury emission factors and temporal patterns of emissions can be found elsewhere (*25*).

Materials and Methods

The study was conducted in May and June of 2006 in the combustion facility of the USFS FSL (*23, 26–30*). The facility consists of a large combustion chamber (12.5 × 12.5 × 22 m (L × W × H)) with a 3.6 m diameter inverted funnel opening extending 2 m above a fuel bed connected to a 1.6 m diameter exhaust stack which is vented through the ceiling. A sampling platform surrounds the smoke stack at 17 m elevation where all measuring equipments for sampling of smoke are deployed. Approximately 250 g of fuels were placed directly on a white ceramic plate and ignited with a pilot light or a propane torch. Foliage, branches, and leaf litter were collected from tree and shrub species from various locations in the U.S., including Ponderosa Pine, Lodgepole Pine, Southern Longleaf Pine, Chamise, Common Manzanita, and Douglas Fir. Both fresh and air-dried fuel material was used to represent fuels with a range of different fuel moisture contents. Table 1 summarizes information on used fuels.

GEM was analyzed using a 2537A gaseous elemental mercury analyzer (Tekran Inc., Toronto, Canada) at 2.5 min sampling intervals and a detection limit of <0.1 ng m^{-3}. Smoke samples were drawn through ¼ inch Teflon tubing, two Teflon filter packs with 2 μm and 0.2 μm pore size Teflon membranes to remove particles, and a soda lime trap. The instrument was operated with a flow rate of 1.5 L min^{-1} and calibrated twice daily (before and after combustion experiments) using an internal mercury permeation source. No changes in the performance of the gold traps to capture mercury were observed during the experiment as evident by constant detector readings during calibration. Based on the increased surface area in the sampling path caused by the use of two filters and a soda lime trap, we expect that the Tekran measured predominantly GEM. GEM emissions were calculated by determining a baseline GEM level prior to the start of combustion and calculating GEM enhancement during the combustion. PHg was collected onto clean, preheated (>800 °C; 8 hours) 47 mm diameter Pallflex Tissuquartz filters (Pallflex 2500 QAT-UP, Pall Life Sciences, Ann Arbor, MI; collection efficiency for 0.3 μm particles: 99.9%) using a flow rate of 50 standard liters per minute. Emissions from three replicate burns were sampled onto one single filter to assure sufficient filter loading. Three additional filters each were used as dynamic blanks (same flow rate as the sample filters) and as static blanks (i.e., connected to the sampling setup for 5 minutes with no airflow). Filter loadings of dynamic and static blanks for PHg were not significantly different and averaged 58 ± 52 pg, which was deducted from all sample filters for calculation of PHg emissions. Analysis of the PHg filters was performed by Frontier Geosciences, Inc. in Seattle. Filters were digested with 40 mL of 10% BrCl and analyzed using $SnCl_2$ reduction, dual gold amalgamation, and cold vapour atomic fluorescence spectrometry detection. Certified Reference Material resulted in a recovery rate of 98.9%.

Smoke particulate matter (PM) was collected on 47 mm diameter Teflon-membrane and quartz-fiber filters for the quantification of mass (by gravimetry) and organic carbon (OC), elemental carbon (EC), and total carbon (TC = OC + EC) concentrations. OC and EC were determined by the IMPROVE-A protocol (*31*) using a DRI model 2001 carbon analyzer. Additional PM speciation was performed using X-ray fluorescence (for elements), ion chromatography (for anions), atomic absorption spectroscopy (for soluble sodium and potassium), and automatic colorimetry (for ammonium; ref *32*). Carbon dioxide (CO_2), carbon monoxide (CO), and total hydrocarbon (THC) smoke concentrations were measured by infrared absorption (LI-840, Li-COR Environmental and model 48C, Thermo Electron Corporation) and chemiluminenscence (model 42C, Thermo Electron Corporation) as described in ref *23*. Fuel and ash samples were collected during the experiment, freeze-dried, and homogenized using a stainless steel coffee mill, and C contents in fuels and ash were measured using an elemental analyzer (CNS-2000, LECO Corp.). Total mercury in fuel and ash samples were measured using a total mercury analyzer (MA-2000; Nippon Corporation) measured in triplicate (CV of triplicates <10% unless concentrations lower than 10 μg/kg). Smoke-based mercury emissions were calculated by multiplication of measured

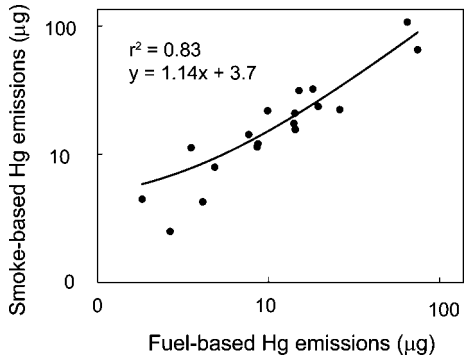

FIGURE 1. Comparison between fuel-based mercury (Hg) emissions and emissions based on measurements in smoke stack (smoke-based). Fuel-based mercury emissions are calculated by measured fuel and ash mercury concentrations multiplied by mass losses during combustion. Smoke-based mercury emissions are calculated as measured mercury/C emissions ratios (i.e., (GEM + PHg)/(CO_2 + CO + THC) multiplied by C mass losses during combustion.

mercury/C emissions ratios (i.e., (GEM + PHg)/(CO_2 + CO + THC) multiplied by mass loss of C in fuels (based on fuel and ash mass and C contents). Fuel-based mercury emissions were calculated by measured fuel and ash mercury concentrations multiplied by mass losses during combustion.

Results

GEM and PHg Detection in Smoke. Baseline GEM concentration in the exhaust smoke stack, i.e., concentrations prior and after the burns when no combustion occurred, averaged 7.5 ± 1.4 ng m^{-3} (mean ± standard deviation; n = 60) indicating enhanced mercury levels inside the facility as compared to outside concentrations. Nonetheless, GEM sampling of smoke during burns yielded well detectable GEM enhancement levels compared to laboratory background concentrations for all 60 individual burns (e.g., enhanced by an average of 3.3 ± 3.1 ng m^{-3} and 2.2 ± 3.1 ng m^{-3}, respectively, for the first and second 2.5 intervals). GEM enhancements decreased during later stages of the combustion with no detectable levels after 15 minutes. Detection of PHg proved more difficult in spite of collection of three replicate burns onto one common quartz filter. Half of the samples showed low PHg values close or below the detection limit. Blank-corrected filter loadings of PHg ranged from −42 to 341 pg per filter (average 85 ± 111 pg/filter). Negative PHg concentrations were due to lower filter loadings of the sampling filters than filter blanks which were deducted thereof, and hence represent no detectable PHg levels. Of the 20 blank-corrected filter loadings, 10 values did not exceed the 90% confidence interval of the blanks (−35 to +35 pg). However, these values were still kept in figures and tables for calculation of fractional PHg contributions, although low PHg values should be viewed as close or below the detection limits.

Average fuel mercury levels across the 60 burns were 30.6 ± 4.3 μg/kg, with fresh biomass fuels showing generally lower mercury levels than air dried samples (Table 1). Measurements of mercury emissions in smoke (GEM + PHg) compared well to emissions calculated based on analyses of total mercury in fuel and ash. Figure 1 shows the correlation between emissions measured by the two methods (P < 0.01; r^2 = 0.83). Emissions estimates based on smoke measurements are 14% higher as compared to emissions based on fuel and ash mercury levels.

Emission Ratios for GEM and PHg and Speciation between GEM and PHg. Mercury levels in smoke (i.e., GEM + PHg) ranged from 80 pg m^{-3} to 2.3 ng m^{-3} (note that these low values represent high concentrations early in combustion diluted by very low concentrations during later combustion phases). Figure 2 shows GEM and PHg emission ratios (ERs), and the fractional contribution of PHg contributions to total mercury emissions for various fuel types. ERs are calculated as excess concentrations of GEM and PHg in smoke in relation to the excess carbon concentrations. GEM ERs were highest in dry fuels (i.e., dry needles, branches, leaves, and rice straw) and lower in fresh fuels. The patterns for PHg ERs were almost reversed, with fresh needles and leaves showing the highest PHg emission ratios (up to 17 ng PHg/g C). Hence, highest PHg fractions were found for the combustion of fresh fuel types (up to 43% of total mercury for fresh needles and 17% for fresh leaves). At the low end were dry fuel types, with dry branches and dry needles showing no detectable PHg emissions (e.g., none of the filter loadings of dry branches was exceeding the 90% confidence interval of the filter blanks). No inherent difference in GEM and PHg ERs, or the fraction of PHg of total mercury was observed among the different plant species.

Factors Affecting Mercury Speciation in Biomass Smoke. Figure 2 suggests a dependency of PHg contributions in biomass smoke on fuel moisture. Figure 3A shows that up to fuel moistures of around 30% (dry mass basis), PHg fractions in smoke remain small (below 5%). At higher fuel moistures, PHg contributions start to increase becoming as high as 48% in fresh lodgepole pine needles. Overall, a linear regression between the PHg fraction and fuel moisture is not significant, but a regression exists when only data points with fuel moisture above 30% are included (P = 0.048; r^2 = 0.41). Hence, there is a threshold of around 30% fuel moisture when PHg contributions become important, with very significant contributions occurring above 50% fuel moisture. Comparison of fuel types differing in fuel moistures (i.e., air-dried and fresh fuel samples) confirms the importance of fuel moisture on PHg contributions (Table 2). In all seven fuels, PHg contributions are higher in fresh fuels as compared to air-dried fuels.

A pronounced and statistically significant correlation (P < 0.01) across all fuel types is observed between PHg emissions and flaming/smoldering combustion ratios (defined as the duration of flaming combustion divided by the duration of smoldering combustion; Figure 3B). Flaming and smoldering phases combustion were assigned visually for each burn with flaming combustion periods characterized when flames were visible and smoldering combustion as periods without visible flames. Figure 3B shows high PHg fractions when combustion was characterized by a prolonged smoldering phase, while prolonged flaming phases resulted in low and often undetectable PHg fractions. The flaming/smoldering ratio accounts for 56% of the variability in observed PHg fractions using a logarithmic regression line.

PHg Mass Concentration in Relation to PM (Particulate Matter) Mass Concentration and Composition. Smoke PHg concentrations correlate significantly (P < 0.01) with PM mass concentrations (Figure 4A) which explains 70% of the variability in observed smoke PHg concentrations. The slope between PHg and PM mass (i.e., 0.089 pg PHg μg^{-1} PM) indicates that PHg accounts for less than 0.1 ppm of observed PM mass. PHg also correlates with organic carbon (OC; P < 0.01; r^2 = 0.64). OC can be separated into subfractions 1−4 (*31*), which are fractions operationally defined by the temperature when they desorb thermally from the quartz-fiber filters in the absence of oxidants (i.e., OC1: 140 °C; OC2: 280 °C; OC3: 480 °C; and OC4: 580 °C). All fractions but OC1 linearly correlated to PHg concentrations, with OC3 and OC4 showing the highest correlation coefficients to PHg (0.58 and 0.55, respectively). There was no statistically significant relationship between PHg and elemental carbon (EC) mass concentrations of PM (Figure 4C). Sulfur (S) mass concentrations, however correlated with measured PHg mass

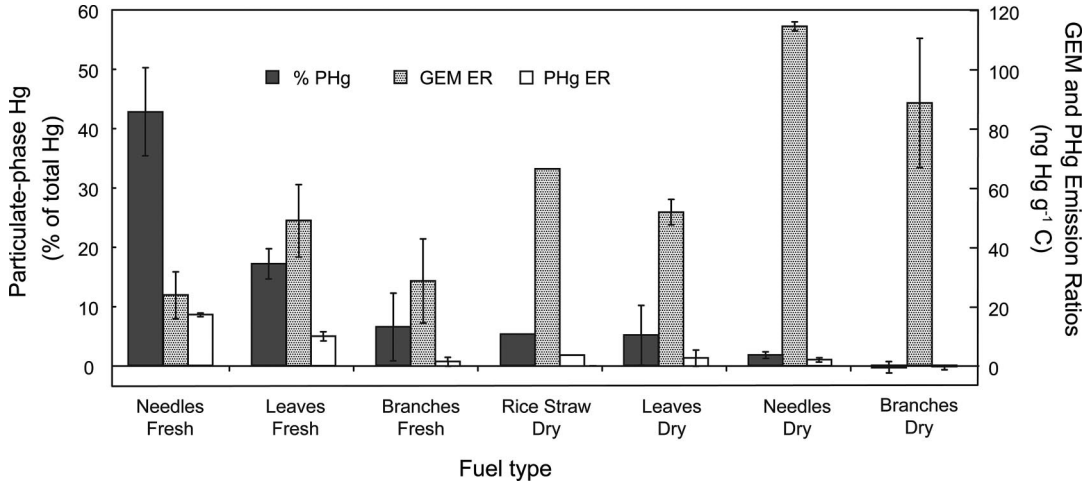

FIGURE 2. Hg emission ratios (in ng Hg g^{-1} carbon; right axis) measured in biomass smoke for gaseous elemental (GEM; gray bars) and particulate-phase (PHg; white bars) mercury for different groups of dry and fresh fuels. Black bars represent the percentages of PHg of total mercury (i.e., GEM + PHg; left axis) for the respective fuel groups.

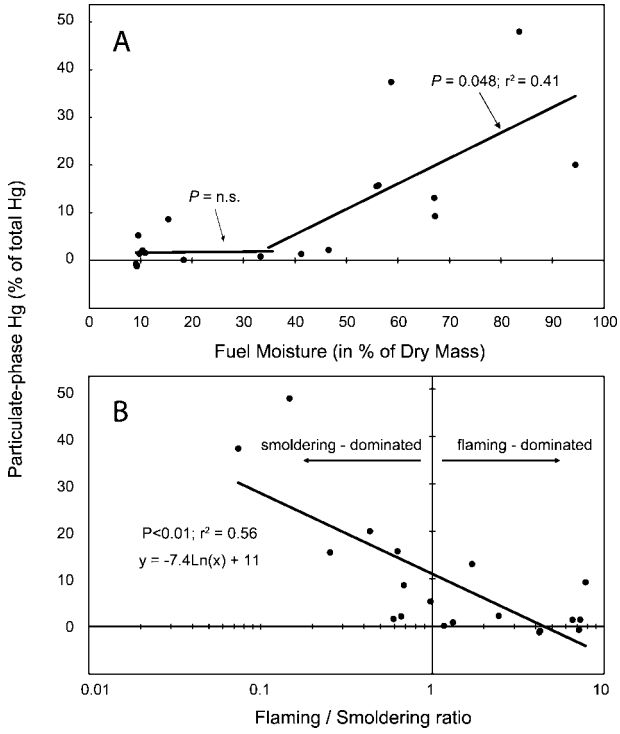

FIGURE 3. A. Percentage of particulate-phase mercury (PHg) of total mercury emissions (i.e., GEM + PHg) as a function of fuel moisture (in % of dry mass) for all measured triplicate burns. B. Same PHg contributions as a function of flaming to smoldering combustion ratios. The flaming/smoldering ratios are calculated as the duration of flaming combustion divided by the duration of smoldering combustion.

concentrations ($P < 0.01$; $r^2 = 0.46$; Figure 4D), a correlation which remained when data points with highest S levels and levels below detection limits where removed (insert in Figure 4D; $r^2 = 0.49$). No significant relationship between chlorine concentrations and PHg was observed.

Discussion

GEM and PHg Emissions and Speciation. Mercury concentrations of fresh fuel materials were close to commonly observed Hg levels reported in literature (i.e., plant foliage concentrations of 24 $\mu g\,kg^{-1}$ (*11*). Dried fuel materials showed considerably higher mercury contents which we attribute to collection of air dried fuels in the field which were exposed to additional deposition during drying. Sampling of smoke from laboratory biomass burning yielded well detectable levels of GEM, but detection of PHg proved more difficult. Comparison of mercury emissions based on smoke stack measurements (i.e., GEM + PHg) with emissions based on fuel and ash mercury analyses and mass losses (Figure 1), however, show a good correlation providing high confidence in measured smoke emission patterns. Reasons for the 14% higher mercury emission estimate in the smoke stack may be due to overestimation of the mercury/C ratio, which was calculated only on the basis of volatile C emissions. These did not include PM-related C losses which can account to a few percent of total C losses. Regardless, the higher estimates of the smoke stack measurements indicate no losses in gold trap mercury collection efficiency of the mercury analyzer during the smoke measurements.

The main objective of this study is to characterize mercury speciation in biomass smoke and to identify key factors controlling speciation. Results presented in Figure 2 show that PHg contributions in smoke of biomass combustion range from nondetectable amounts to almost half of total mercury emissions. PHg emissions and speciation of emissions were independent of the total mercury contents in fuels or the total loss of mercury during combustion, which shows that the formation of PHg is unrelated to the available pool of mercury. The variable PHg emissions support Friedli et al.'s (*3*) notion that evolution of PHg is fuel specific. However, it is important to note that PHg contributions were not inherent to plant species nor were they related to specific fuel types (e.g., leaves versus branches). Fresh needles, leaves, and branches showing higher PHg emissions than dried samples of the same fuels (Table 2) indicate that fuel moisture is an important variable in speciation of emissions. PHg contributions, however, become important only above a threshold value of about 30% fuel moisture (dry mass basis; Figure 3A). The high PHg contributions measured in this study were higher than any values reported in the published literature (e.g., 13% in refs *3*,*10*, and *14*) which might be due to combustion of very wet fuels. In fact, to incinerate some of the wet types of fuels, fuels had to be reignited at times using a small propane torch and/or kept warm with a 500 W electrical coil to assure continuous combustion of the fuels. The fact that some of the high PHg emissions occurred in untorched—albeit high in moisture—fuels suggest no influence of torching on emission speciation.

Fire Properties and Mercury Speciation. Fire properties such as flaming and smoldering combustion show a strong influence on the speciation of mercury emissions (Figure

TABLE 2. Percentage of PHg of Total Mercury Measured in Smoke Compared in Air Dried and Fresh Samples of the Same Fuels[a]

fuel type	fuel moisture low (%)	PHg (in % of total Hg)	fuel moisture high (%)	PHg (in % of total Hg)
ponderosa pine needles	10	1.77	59	37.42
ponderosa pine branches (small)	9	−0.96	47	2.21
ponderosa pine branches (large)	9	−1.24	67	9.28
chamise leaves	15	8.64	56	15.77
chamise branches	33	0.83	41	1.35
manzanita leaves	56	15.57	94	20.04
manzanita branches	18	0.11	67	13.12

[a] Fuel moistures are expressed in percent of dry mass.

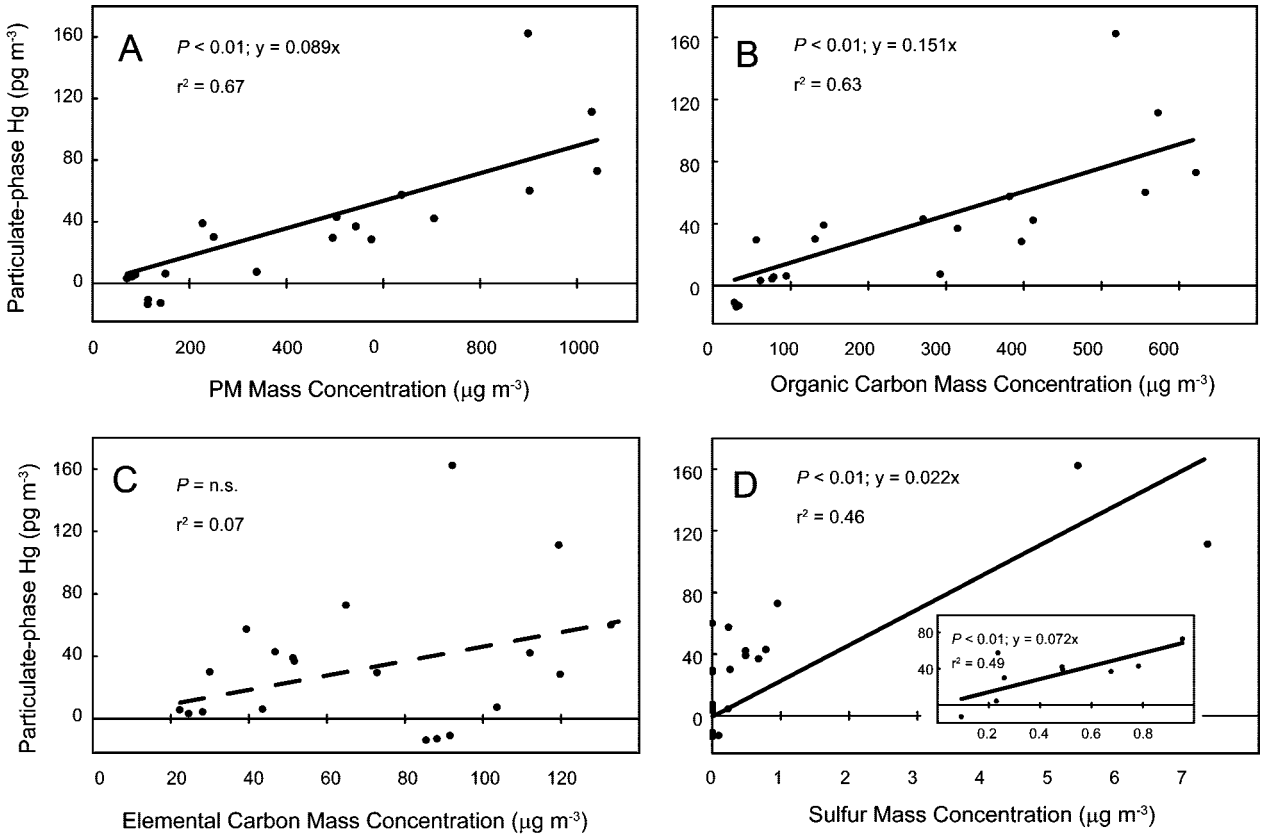

FIGURE 4. A. Scatter plots and linear regressions of particulate-phase Hg (PHg) mass concentrations and particulate matter (PM). B. Scatter plots and linear regressions of PHg mass concentrations and particulate organic carbon (OC) mass concentrations. C. Scatter plots and linear regressions of PHg mass concentrations and particulate elemental carbon (EC) mass concentrations. D. Scatter plots and linear regressions of PHg mass concentrations and particulate sulfur (S) mass concentrations.

3B), and it is very likely that this effect is caused by the fuel moisture contents. Smoldering-dominated combustion increased PHg emissions while flaming-dominated burns showed low and often insignificant PHg contributions. Given that fires are very dynamic with smoldering and flaming combustion present simultaneously, we speculate that the dependence of PHg emission on combustion phase might be even more pronounced if pure flaming and smoldering combustion phases can be achieved. A lower temperature surface reaction during smoldering combustion leads to incomplete oxidation of carbon and, hence, to higher contributions of CO and other partially oxidized pyrolysis products (*33*–*35*). Carbonaceous aerosols emitted during the flaming phase are dominated by fractal-like EC chain aggregates, whereas smoldering phase aerosols are dominated by white near spherical OC particles (e.g., ref *27*). Higher PHg contributions in smoldering-dominated fires in this study are consistent with higher OC emissions during this combustion phase (see also below). Hence, the partition between GEM and PHg is likely influenced by combustion temperature which is the confounding factor for OC formation.

PHg Concentrations in Relation to PM Mass Concentrations and Composition. Smoldering combustion dominates—or at least matches—PM emissions compared to flaming combustion for most fuels although only a minor fractions of fuel mass may be consumed during smoldering combustion (*23*). The observed correlation of PHg to PM and OC mass concentrations, particularly OC3 and OC4 fractions, suggests that processes that lead to the formation of OC aerosols may also be responsible for the formation of PHg. When smoke cools and dilutes, low vapor pressure organic species condense onto preexisting smoke particles forming OC-coated aerosols (*36*). We hypothesize that a similar process may be responsible for the formation of PHg during biomass combustion, i.e., that volatile mercury species condense onto aerosol particles rapidly during cooling under conditions similar to those observed for the formation of OC aerosols. High gas-particle partitioning coefficients reported

for reactive mercury (up to 600 m^3 μg^{-1}; ref *37*) support the notion that PHg could readily form via condensation of RGM, which should also explain a lack of significant amounts of RGM in cooled biomass smoke (*10*). According to the desorption temperature of OC2 to OC4—the OC fractions that correlate better with PHg—they likely consist of compounds condensable between 280 and 580 °C. These temperatures are within the range of release temperatures of some mercury species released from soils and organic substrates, for example HgS (240–460 °C) or mercury associated with humic acids (200–330 °C; *38*), which could therefore play a role in PHg formation. Other mercury species show lower release temperatures (i.e., $HgCl_2$: 50–400 °C; GEM: 50−150 °C). A correlation of PHg with S—and a lack thereof with chloride—would be consistent with the involvement of S containing reactive mercury species. The lack of any correlation between EC and PHg mass concentrations (Figure 4C) and the fact that EC is largely emitted during flaming (*23*) indicate that formation of PHg is largely unrelated to the presence of EC aerosols, which potentially might have formed a strong chemisorption with mercury similar to that observed for activated carbon. Certainly, further detailed studies are needed to clarify the formation of PHg during biomass combustion.

Estimate of Global PHg Emission from Wildfires. The data further suggest that estimation of global PHg emissions by wildfires should not be based on existing emission inventories for total mercury given that the partition between GEM and PHg is highly variable. Scaling up emissions based on fuel moisture contents in biomass fuels, on the other hand, would be challenging as we are not aware of detailed fuel moisture inventories of wildfires. We propose to use the observed relationships of PHg mass concentrations to OC and to PM mass concentrations to estimate PHg emissions. Based on the linear slope between PHg and OC concentrations of 150 ng PHg g^{-1} OC and on a global OC emissions inventory from open biomass burning of 25 Tg/yr (*39*), annual PHg emissions would account for 3.8 tons per year. A somewhat higher estimate can be inferred from PM emission inventories (*9*) which estimates global $PM_{2.5}$ emissions (i.e., particles with aerodynamic diameter less than 2.5 μm that constitute the bulk of biomass PM emissions) by wildfires as 58.3 Tg/y. Based on the slope of PHg to PM mass (i.e., 89 ng PHg g^{-1} PM), we estimate global annual wildfire-related PHg emissions to be ∼5.2 tons. These estimates are only in a few percent range of total mercury emission estimates (i.e., 100−1000 Mg yr^{-1}, see Introduction) but may nonetheless be very important for local and regional deposition loads given the 10 times higher deposition velocity of PHg as compared to GEM.

We conclude that the majority of mercury emissions occurs as GEM but that PHg emissions from wildfires can be very important in the presence of fresh wildland fuels with high fuel moisture content (>30% of dry mass). High particulate-phase mercury emissions can be expected especially during smoldering−combustion processes and in fires with high emissions of OC and/or PM mass. As is the case with total mercury emissions, predicted increases in the occurrence of wildfires in this century due to global change (e.g., ref *40*) may increase the importance of these natural emissions on a global scale.

Acknowledgments

We thank the staff of the FSL for their hard work and hospitality in Missoula, Montana. We thank R. Chakrabarty, K. Lewis, and R. Higgins for help with filter sampling and laboratory analysis. We are grateful to J. Chow at the Desert Research Institute and her laboratory for analyses of Teflon and quartz-fiber filters. Funding for collection and analyses of mercury was provided by the National Science Foundation grant ATM-0632780. This research was also supported by the Joint Fire Science Program (JFSP) through the U.S. National Park Service (NPS) project no. J8R07060005. The Tekran 2537A instrument was funded by DRI's EVPR Research Enhancement Program. PM chemical analysis was, in part, supported by the California Air Resource Board grant 04–307.

Literature Cited

(1) Artaxo, P.; Calixto de Campos, R; Fernandes, E. T.; Martins, J. V.; Xiao, Z; Lindqvist, O.; Fernández-Jiménez, M. T.; Maenhaut, W. Large scale mercury and trace element measurements in the Amazon basin. *Atmos. Environ.* **2000**, *34*, 4085–4096.

(2) Brunke, E.-G.; Labuschagne, C.; Slemr, F. Gaseous mercury emissions from a fire in the Cape Peninsula, South Africa, during January 2000. *Geophys. Res. Lett.* **2001**, *28*, 1483–1486.

(3) Friedli, H. R.; Radke, L. F.; Lu, J. Y. Mercury in smoke from biomass fires. *Geophys. Res. Lett.* **2001**, *28*, 31223–3226.

(4) Sigler, J. M.; Lee, X.; Munger, W. Emission and long-range transport of gaseous mercury from a large-scale Canadian boreal forest fires. *Environ. Sci. Technol.* **2003**, *37*, 4343–4347.

(5) Veiga, M. M.; Meech, J. K. A.; Onante, N. Mercury pollution from deforestation. *Nature* **1994**, *368*, 816–817.

(6) Engle, M. A.; Gustin, M. S.; Johnson, D. W.; Murphy, J. F.; Miller, W. W.; Walker, R. F.; Wright, J.; Markee, M. Mercury distribution in two Sierran forest and one desert sagebrush steppe ecosystem and the effects of fire. *Sci. Tot. Environ.* **2006**, *367*, 222–233.

(7) Turetsky, M. R.; Harden, J. W.; Friedli, H. R.; Lannigan, M.; Payne, N.; Crock, J.; Radke, L. Wildfires threaten mercury stocks in northern soils. *Geophys. Res. Lett.* **2006**, *33*, L16403.

(8) Ebinghaus, R.; Slemr, R.; Brenninkmeijer, C. A. M.; van Velthoven, P.; Zahn, A.; Hermann, M.; O'Sullivan, D. A.; Oram, D. E. Emissions of gaseous mercury from biomass burning in South America in 2005 observed during CIRIBIC flights. *Geophys Res. Lett.* **2007**, *34*, L008813.

(9) Andreae, M. O.; Merlet, P. Emission of trace gases and aerosols from biomass burning. *Global Biogeochem. Cycles* **2001**, *15*, 955–966.

(10) Friedli, H. R.; Radke, L. F.; Lu, J. Y.; Banic, C. M.; Leaitch, W. R.; MacPherson, J. I. Mercury emissions from burning of biomass from temperate North American forests: Laboratory and airborne measurements. *Atmos. Environ.* **2003a**, *37*, 253–267.

(11) Grigal, D. F. Inputs and outputs of mercury from terrestrial watersheds: A review. *Environ. Rev.* **2002**, *10*, 1–39.

(12) Obrist, D. Atmospheric mercury pollution due to losses of carbon pools. *Biogeochemistry* **2007**, *85*, 119–123.

(13) Obrist, D.; Conen, F.; Vogt, R.; Siegwolf, R.; Alewell, C. Quantification of elemental Hg^0 exchange using $^{222}Rn/Hg^0$ accumulation in the stable nocturnal boundary layer. *Atmos. Environ* **2006**, *40*, 856–866.

(14) Friedli, H. R.; Radke, L. F.; Prescott, R.; Bobbs, P. V.; Sinha, P. Mercury emissions from the August 2001 wildfires in Washington State and an agricultural waste fire in Oregon and atmospheric mercury budget estimates. *Global Biogeochem. Cycles* **2003b**, *17* (2), 1039.

(15) Seigneur, C.; Vijayesaghavan, K.; Lohman, K. Atmospheric mercury chemistry: Sensitivity of global model simulations to chemical reactions. *J. Geophys. Res.* **2006**, *111*, D22306.

(16) Seigneur, C.; Vijayesaghavan, K.; Lohman, K.; Karamchandani, P.; Scott, C. Global source attribution for mercury deposition in the United States. *Environ. Sci. Technol.* **2004**, *38*, 555–569.

(17) Schroeder, W. H.; Munthe, J. Atmospheric mercury—An overview. *Atmos. Environ.* **1998**, *32*, 809–822.

(18) Weiss-Penzias P.; Jaffe, D.; Swartzendruber, P.; Hafner, W.; Chand, D. Quantifying Asian and biomass burning sources of mercury using the Hg/CO ration in pollution plumes observed at the Mount Bachelor Observatory. *Atmos. Environ.* **2007**, *41*, 4366−5479.

(19) Schroeder, W. H.; Anlauf, K. G.; Barrie, L. A.; Lu, J. Y.; Steffen, A. Artic springtime depletion of mercury. *Nature* **1998**, *394*, 331–332.

(20) Ebinghaus, R.; Kock, H. N.; Temme, C.; Einax, J. W.; Lowe, A. G.; Richter, A.; Burrows, J. P.; Schroeder, W. H. Antarctic springtime depletion of atmospheric mercury. *Environ. Sci. Technol.* **2002**, *36*, 1238–1244.

(21) Peleg, M.; Matveev V.; Tas E.; Luria M.; Obrist D. Mercury depletion events in the troposphere in Mid-Latitudes at the Dead Sea, Israel. *Environ. Sci. Technol.* [Online early access] DOI: 10.1021/es070320j.

(22) Ariya, P. A.; Dastoor, A. P.; Amyot, M.; Schroeder, W. H.; Barrie, L.; Anlauf, K.; Raofie, F.; Ryzhkov, A.; Davignon, D.; Lalonde, J.; Steffen, A. The Arctic: a sink for mercury. *Tellus, Ser. B* **2004**, *56*, 397–403.
(23) Chen, L.-W. A.; Moosmüller, H.; Arnott, W. P.; Chow, J. C.; Watson, J. G. Particle emissions from laboratory combustion of wildland fuels: Emission factors and source profiles. *Environ. Sci. Technol.* **2007**, *41*, 4317–4325.
(24) Lee, S. E.; Schauer, J. J.; Sheesley, R. J.; Naeher, L. P.; Meinhardi, S.; Blake, D. R.; Edgerton, E. S.; Russell, A. G.; Clements, M. Gaseous and particulate emissions from prescribed burning in georgia. *Environ. Sci. Technol.* **2005**, *39*, 9049–9056.
(25) Obrist, D.; Moosmüller, H. Mercury emissions from laboratory combustion of wildland fuels: Emission factors, and source profiles. In preparation.
(26) Christian, T. J.; Kleiss, B.; Zokelson, R. J.; Holyinger, R., Crutzen, P. J.; Hao, W. M.; Shirai, T.; Blake, D. R. Comprehensive laboratory measurements of biomass-burning emissions: 2. First intercomparison of open-path FTIR, PTR-MS, and GC-MS/FID/ECD. *J. Geophys. Res.* **2004**, *109*,doi:10.1029/2003JD003874.
(27) Chakrabarty, R. K.; Moosmüller, H; Garro, M. A.; Arnott, W. P.; Walker, J. W.; Susott, R. A.; Babbitt, R. E.; Wold, C. E.; Lincoln, E. N.; Hao, W. M. Particle emissions from laboratory combustion of wildland fuels: Particle morphology and size. *J. Geophys. Res.* **2006**, *111*, 10.1029/2005JD006659.
(28) Chen, L.-W. A.; Moosmüller, H.; Arnott, W. P.; Chow, J. C.; Watson, J. G.; Susott, R. A.; Babbitt, R. E.; Wold, C. E.; Lincoln, E. N.; Hao, W. M. Particle emissions from laboratory combustion of wildland fuels: *In-situ* optical and mass measurements. *Geophys. Res. Lett.* **2006**, *33*,doi:10.1029/2005GL024838.
(29) Mazzoleni, L. R.; Zielinska, B.; Moosmüller, H. Emissions of levoglucosan, methoxy phenols, and organic acids from prescribed burns, wildland fuels, and residential wood combustion. *Environ. Sci. Technol.* **2007**, *41*, 2115–2122.
(30) Goode, J. G.; Yokelson, R. J.; Susott, R. A.; Ward, D. E. Trace gas emissions from laboratory biomass fires measured by Fourier transform infrared spectroscopy: Fires in grass and surface fuels. *J. Geophys. Res.* **1999**, *104*, 21237–21245.
(31) Chow, J. C.; Watson, J. G.; Chen, L.-W. A.; Chang, M. C. O.; Robinson, N. F.; Trimble, D.; Kohl, S. The IMPROVE_A temperature protocol for thermal/optical carbon analysis: Maintaining consistency with a long-term database. *J. Air Waste Manage. Assoc.* **2007**, *57*, 1014–1023.
(32) Chow, J. C. Critical review: Measurement methods to determine compliance with ambient air quality standards for suspended particles. *J. Air Waste Manage. Assoc.* **1995**, *45* (5), 320–382.
(33) Hays, M. D.; Geron, C. D.; Linna, K. J.; Smith, N. D.; Schauer, J. J. Speciation of gas-phase and fine particle emissions from burning of foliar fuels. *Environ. Sci. Technol.* **2002**, *36*, 2281–2295.
(34) Yokelson, R. J.; Griffith, D. W. T.; Ward, D. E. Open-path Fourier transform infrared studies of large-scale laboratory biomass fires. *J. Geophys. Res.* **1996**, *101*, 21067–21080.
(35) Yokelson, R. J.; Susott, R.; Ward, D. E.; Reardon, J.; Griffith, D. W. T. Emissions from smoldering combustion of biomass measured by open-path Fourier transform infrared spectroscopy. *J. Geophys. Res.* **1997**, *102*, 18865–18877.
(36) Reid, J. S.; Koppmann, R.; Eck, T. F.; Eleutrerio, D. P. A review of biomass burning emissions part II: Intensive physical properties of biomass burning particles. *Atmos. Chem. Phys.* **2005**, *5*, 799–825.
(37) Rutter, A. P.; Schauer, J. J. The impact of aerosol composition on the particle to gas partitioning of reactive mercury. *Environ. Sci. Technol.* **2007**, *41*, 3934–3939.
(38) Biester, H.; Scholz, C. Determination of mercury binding forms in contaminated soils: Mercury pyrolysis versus sequential extractions. *Environ. Sci. Technol.* **1997**, *31*, 233–239.
(39) Bond, T. C.; Streets, D. G.; yesber, K. F.; Nelson, S. M.; Woo, J.-H.; Klimont, Z. A technology-based global inventory of black and organic carbon emissions from combustion. *J. Geophys. Res.* **2004**, *109* (D14), D14203.
(40) Fried, J. S.; Torn, M. S.; Mills, E. The impact of climate change on wildfire severity: A regional forecast for northern California. *Climate Change* **2004**, *64*, 169–191.

ES071279N